Musa Acuminata Banana Bunch-Based Activated Carbon for Adsorption of Cu(II) Ions in Aqueous Solution: Kinetic and Isotherm Studies

Muslim, Abrar*+; Thaib, Anwar; Rosnelly, Cut Meurah; Hidayatullah, Muhammad; Riyadh, Muammar, Guswara, Yusupi

Department of Chemical Engineering, Universitas Syiah Kuala, No.7 Jalan Tgk. Syech Abdul Rauf, Darussalam, Banda Aceh, INDONESIA

Kadri, Atikah

Faculty of Chemical Engineering, Universiti Teknologi MARA (UiTM), 40450 Shah Alam, MALAYSIA

ABSTRACT: *Activated Carbon prepared from Musa Acuminata Banana Bunch (AC-MABB) was proposed in this study. The active sites and morphology structure of three types of the AC-MABB were analyzed using FT-IR and SEM, respectively. The effect of independent variables namely contact time, Cu(II) ions concentration in solution, NaOH activator concentration, initial pH, and temperature on adsorption capacity of the AC-MABB were investigated through batch mode experiments. The Cu(II) ions adsorbed onto the AC-MABB showed excellent fitting to the pseudo-second-order adsorption kinetic with a correlation coefficient value of 0.999. Meanwhile, it followed Langmuir isotherm with coefficient values of 0.981 and 0.991 at 27 and 57 ºC, respectively. The optimum adsorption condition for 1 g of the AC-MABB was observed to be under 0.4 M NaOH activation atmosphere and, stirred at initial pH of 5 with a speed of 100-rpm and a pressure of 1 atm. The maximum Cu(II) ions adsorption capacity based on Langmuir was identified approximately equal to 40.322 and 46.082 mg/g at 27 and 57 ºC, respectively.*

KEYWORDS: *Musa Acuminata; Bunch; Activated carbon; Capacity; Kinetics; Isotherm.*

INTRODUCTION

The development of industries can have negative impacts on the environment. Extensive agricultural activities, mining operations, and refining of petroleum might release organic and inorganic pollutants including heavy metals to streams, rivers, lakes, and groundwater [1-6]. Cu(II) ions are one of the pollutants in the water bodies and commonly exist in industrial wastewater [7].

It is dangerous to humans as it may cause tissues and organs to malfunction [8, 9].

Among other chemical processes, adsorption is a promising technology for the removal of heavy metals in soil and wastewater as it is more effective, environmentally friendly, and easily applicable [10-12]. It is also economically friendly especially when it uses a low-cost

lignocellulosic materials-based as the adsorbents [13]. Some adsorbents highlighted in the previous studies have been prepared from rice husk [14], sunflower leaves [15], wheat straw [16], Cinnamomum camphora leaves [17], areca catechu shell [18], watermelon [19] are used for Cu(II) ion adsorption.

In the global scene, it is expected that the activated carbon market would reach approximately 2.78-kilotons by 2022 [20], thus offering tremendous opportunity in producing a better type of adsorbents. A great deal of research investigations, as reported in the literature has been directed towards the application of lignocellulosic materials as the adsorbent for Cu(II) ions such as hazelnut husks [21], pecan shell [22], hazelnut shell [23], cassava peel [24], Tunisian date stones [25], corncob [26], Australian pine cones [27], Pithecellobium jiringa shell [28], myristica fragrans shell [29] and areca catechu stem [30]. Banana Empty Fruit Bunch (BEFB) has been used as a raw material of activated carbon to reduce methylene blue. The carbon was impregnated with H_3PO_4 and KOH [31]. The same acid was used to the BEFB activate carbon for hydrothermally treated-based activated carbon for Zn(II) and Pb(II) adsorption [32]. The type of banana was not mentioned in the previous studies. Meanwhile, there are almost 1,000 types of bananas in the world, and the global production has 47% of Musa Acuminata banana which is 50 billion tonnes/year [33]. Therefore, it is still necessary to prepare activated carbon from Musa Acuminata Banana Bunch (MABB) for Cu(II) adsorption. Pyrolysis of the MABB in a tube furnace with nitrogen injected, and activating banana bunch carbon using NaOH has not been investigated in the previous studies.

The main objective of this work is to propose an Activated Carbon (AC) prepared from the MABB (AC-MABB) for Cu(II) adsorption. The morphology structure and chemical functional group of the active sites of the AC-MABB were analyzed and characterized. The effects of independent variables i.e. contact time, the concentration of NaOH, initial concentration of Cu(II) ions in solution, pH, and temperature on the adsorption capacity were investigated. Isotherm and kinetic adsorption studies were conducted. The maximum Cu(II) ions adsorption capacity by various activated carbons was highlighted to compare.

EXPERIMENTAL SECTION
The AC–MABB preparation and analyses

The common method to prepare activated carbon [27,29,38,39] was applied in the AC-MABB production. The 1 kg of MABB was dried under the sun for 7 days at 30 °C (± 1 °C) on average [28]. The dried MABB was ground and sieved to 60-80 mesh size. Then, it was pyrolyzed in a tube furnace (TF 120, 300-1500 °C from Human Lab Inc. Korea) with nitrogen injection at 5 mL/min [30] from an initial temperature of 28 °C (± 1 °C) to final carbonation temperature of 450 °C at a heating rate of 45 °C/min. The sample was kept for 1 hour at 450 °C for physical activation. This activated carbon was labeled as the AC-MABB0, which refers to a sample without chemical activation. After reaching 27 °C, the material of 0.03 kg was activated chemically using 300 mL of NaOH 1 M (97% pure, Aldrich) in a 500-mL beaker glass stirred at 100 rpm (Magnetic Mini, Compact Type HI 180-2 F) for 24 h at 28 °C (± 1 °C) and this sample was denoted as AC-MABB1. This was repeated for the other two runs of the activation process with 0.7 and 0.4 M of NaOH to produce two (2) types of the AC-MABB denoted as AC-MABB0.7 and AC-MABB0.4, respectively. Then, each AC-MABB sample was washed several times using Reverse Osmosis (RO) water until the neutral pH of 7 (± 0.1) was reached.

The AC-MABB chemical functional groups were analyzed using Fourier Transform Infrared Spectroscopy (FT-IR, IR Prestige 21 from Shimadzu, made in Japan). KBr pellets at 0.1% of the sample were used to obtain the AC-MABB transmission spectra at a range of 400–4000 cm^{-1}. The AC-MABB surface morphology was analyzed using Scanning Electron Microscopy (SEM, Jeol-JSM-6360LA, made in Japan).

A stock Cu(II) ions solution of 2 L at 500 mg/L was made using the previous method [28]. The real Cu(II) ions concentration was determined using an Atomic Absorption Spectrophotometer (AAS, type AA-6300 from Shimadzu, made in Japan) while the initial Cu(II) ions concentration for each experiment was determined by dilution [30].

Experiments of Cu(II) ions adsorption

All the adsorption experiments were conducted in batch mode [29,30]. The AC-MABB and solution system consisted of 100 mL Cu(II) ions solution, 1 g of adsorbent (AC-MABB1, AC-MABB0.7, AC-MABB0.4, or AC-MABB0) in a 200-mL Erlenmeyer flask at 100-rpm steering speed

and 1 atm. The adsorption capacity of the AC-MABB was obtained over the initial Cu(II) ions concentration (5.29–511.32 mg/L), NaOH concentration (0.4–0.7 M), pH (3–7), and adsorption temperature (27–57 °C). The adsorption kinetics and isotherm of Cu(II) ions were determined at the optimum condition. The AC-MABB adsorption capacity was also compared to various activated carbons from previous studies.

RESULTS AND DISCUSSION

The transmission spectra of the AC–MABB

The transmission spectra of the AC-MABB1, AC-MABB0.7, AC-MABB0.4, and AC-MABB0 are shown in Fig. 1. The AC-MABB0 consists of 4 functional groups with transmission spectra in the range of 400–4000 cm^{-1}. It is observed that there are two weak bands with the peaks at 3701 and 3662 cm^{-1} which are in the range of 3508-3712 cm^{-1} are associated with hydroxyl groups of O-H stretch [19, 27]. On the other hand, a wide band with three peaks at 2975, 2878, and 2815 cm^{-1} are identified to represent alkenes of C–H stretch in the wavenumber range of 2700-2980 cm^{-1}. Another wide band with two peaks at 1689 and 1520 cm^{-1} matches the aromatic rings of the C=C stretch in a wavenumber range of 1508-1712 cm^{-1} [34]. A strong band of C–H symmetrical and asymmetrical stretching is observed in a wavenumber range of 1321-1452 cm^{-1}. The last one was a weak band of C–C stretch at 400-700 cm^{-1} with a peak at 569 cm^{-1} [35].

Overall, chemical activation using NaOH shipped down the transmission spectra of the AC-MABB0 leading to the decrease of all the transmittance peaks. Chemical activation using NaOH also weakened the C–H and C=C stretch peaks, and it might cause alkenes and aromatic compounds in the activated carbon being released from the AC-MABB0 leading to more porous being formed on the surface of the AC-MABB1, AC-MABB0.7, AC-MABB0.4. Interesting to note that decreasing NaOH concentration from 1 and 0.7 M to 0.4 M, resulted in the incline of O-H stretching peaks. This means that hydroxyl groups formed more on the surface of AC-MABB0.4 as compared to AC-MABB1 and AC-MABB0.7, and this might result in more active sites of hydroxyl groups being formed on the AC-MABB0.4 for chemical adsorption of Cu(II) ions.

Surface morphology of the AC–MABB

Surface morphology of the AC-MABB0, AC-MABB0.4, and AC-MABB1 are shown in Figs. 2(a), (b) and (c),
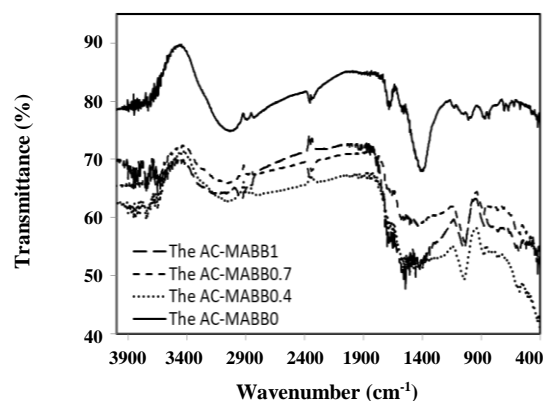
Fig. 1: The FT-IR spectra of the AC-MABB.

respectively. It is shown in Figs. 2, that the AC-MABB0 wall is thicker as compared to the AC-MABB0.4 and AC-MABB1. It is also observed that AC-MABB0.4 is more porous as compared to AC-MABB0. This observation is reasonable because, from the FT-IR perspective, alkenes and aromatic compounds in the activated carbon were released from the AC-MABB0 leading to more pores being formed on the surface of the other samples.

NaOH acted as dehydrating agent to dehydrate water and create more pores as observed in AC-MABB0.4 [27]. On the other hand, AC-MABB1 showed the clearest surface where there were almost no impurities on the AC-MABB1 compared to the AC-MABB0.4. However, less porous was observed on the AC-MABB1 compared to the AC-MABB0.4. This shows that a high concentration of NaOH might break the activated carbon wall including the pores [36] resulting in fewer pores observed in AC-MABB1. Overall, AC-MABB0.4 showed the best surface morphology, and the AC-MABB0.4 adsorption capacity is expected to be highest compared to AC-MABB0 and AC-MABB1.

Effect of contact time on adsorption capacity

The Cu(II) ions adsorption capacity on the AC-MABB04 and AC-MABB1 over contact time is highlighted in Fig. 3. Both activated carbons, the AC-MABB1 and AC-MABB0.4 show the same trend where both increased sharply for the first 15-min contact time. The absorption capacity was approximately 21.60 and 24.99 mg/g for the AC-MABB1 and AC-MABB0.4, respectively at 15-min contact time. It increased gradually to 22.29,
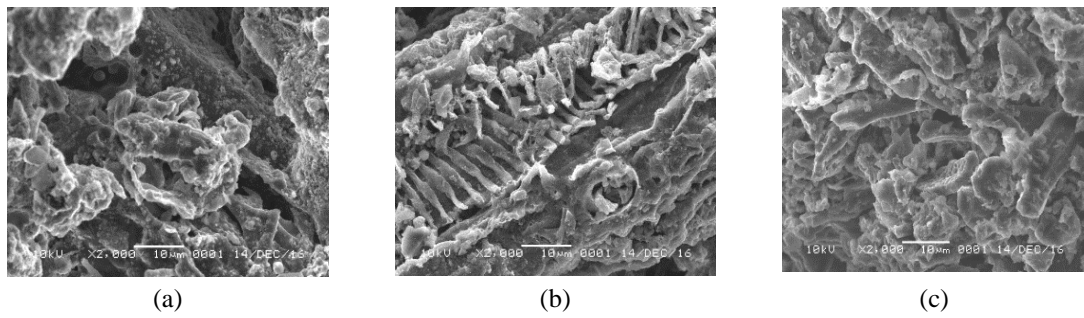
Fig. 2: The SEM micrographs of (a) the AC-MABB0, (b) AC-MABB0.4 (c) the AC MABB1.
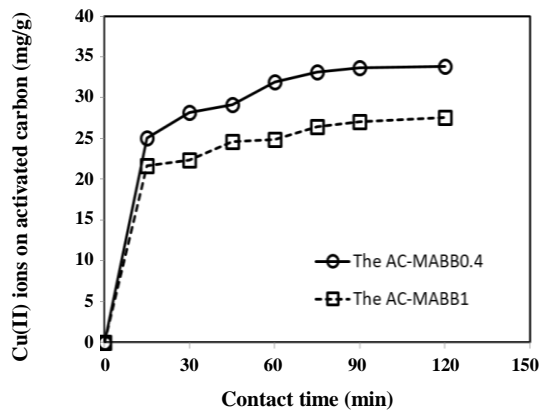

Fig. 3: Cu(II) ions on activated carbon over contact time.

Fig. 4: Cu(II) on activated carbon over initial Cu(II) ions concentration.

24.62, 24.84, and 26.42 mg/g at 30, 45, 60, and 75-min contact time, respectively for the AC-MABB1, and 28.17, 29.15, 31.89, 33.15 mg/g, respectively for the AC-MABB0.4. The AC-MABB1 adsorption capacity changed a little bit at 90 and 120-min contact time, which was 27.03 and 27.56 mg/g, respectively. It was 33.66 and 33.81 mg/g, respectively for the AC-MABB0.4. Therefore, the equilibrium time was 120-min, and it was set for further isotherm experiments. Both samples showed a gradual increment in the absorption capacity after the contact time of 15 minutes and onwards until each sample reached its plateau at the contact time of 75 minutes and 90 min. up to the contact time of 120 minutes for AC-MABB0.4 and AC-MABB1 respectively. Thus, it is reasonable to take 120 minutes as the equilibrium time and use it in the following isotherm experiments. Fig. 3 shows clearly that it was an exponential growth over contact time and it was in accordance with the previous finding [19,27,29,37].
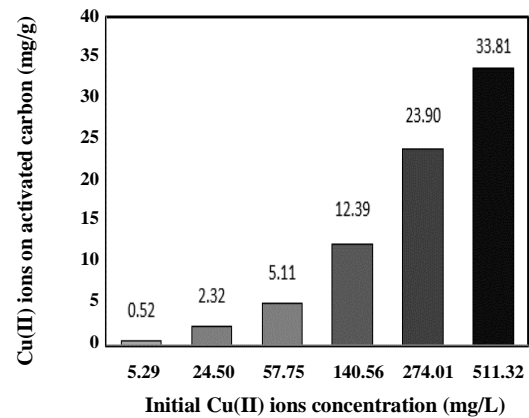
Effect of initial adsorbate on adsorption capacity

The initial Cu(II) ions concentration affected on adsorbent adsorption capacity depends on the adsorbent used. It was reported that the adsorption capacity of both activated carbon decreased for the increasing initial adsorbate concentration from 1 to 14 mg/L using activated Areca catechu shell [19], and it increased for the increase from 6.465 to 645.540 mg/L [29]. In the present study, the same typical result for AC-MABB0.4 was obtained as shown in Fig. 4. The Cu(II) adsorption is gradually increased from 0.52 to 5.11 mg/g for the increment of the initial Cu(II) ion concentration from 5.29 to 57.75 mg/L, respectively. Then, it inclined sharply to the amount of 12.39, 23.90, and 33.81 mg/g for the initial Cu(II) ions concentration of 140.56, 274.01, and 511.32 mg/L, respectively, and this trend is almost the same as it was reported in the previous study [38]. It could be because the range of initial Cu(II) ions concentration was not still wide enough to let all the active sites on activated carbon being occupied by Cu(II) ions reach their steady-state [39].

Effect of NaOH concentration on adsorption capacity

Fig. 5 shows the adsorption capacity of the activated carbon against the difference activating NaOH concentration. As revealed in Fig. 5, the adsorption capacity of AC-MABB0.4 increased from 33.81 to 33.30 and 27.56 mg/g when the concentration of NaOH increases from 0.4 to 0.7 and 1 M, respectively. This finding was also supported by the FT-IR result shown in the previous section where there are more hydroxyl groups were formed on the surface of AC-MABB0.4 as compared to the AC-MABB1 and AC-MABB0.7. It was also shown by the increasing of O-H stretching peaks when the concentration of NaOH is decreased. In addition, the higher the concentration of NaOH agent, it can cause in cracking of C=C stretching leading to broken pores on adsorbent thus lowering the adsorption capacity.

Effect of initial pH on adsorption capacity

In general, the best Cu(II) ions adsorption on adsorbents occurred under acidy and neutral pH conditions [19, 25, 40, 41]. It is reasonable, to avoid $Cu(OH)_2$ solid formation in the alkaline solution before adsorption took place. The effect of initial pH is shown in Fig. 6. The initial pH of Cu(II) ions solution was adjusted by dropping 0.1 M HNO_3, or 0.1 M NaOH solution. As shown in Fig. 6, the Cu(II) ions adsorption on AC-MABB0.4 increased moderately as the pH increased from 3 to 5. Surprisingly, it dropped dramatically to 1.56 mg/g at the pH value of 7. As expected, adding 0.1M NaOH solution to reach pH 7 caused the formation of $Cu(OH)_2$ solid in solution which was indicated by the change of Cu(II) ions solution color from clear blue to whitish blue. The maximum AC-MABB0.4 adsorption capacity was found to be 33.81 mg/g at pH 5 and this is almost similar to the one in the previous study that uses the design expert-based optimization approach [30].

Effect of temperature on adsorption capacity

As shown in Fig. 7, the Cu(II) ions adsorption on AC-MABB0.4 increased linearly from 33.81 to 35.00 and 36.41 mg/g as the temperature increased from 27 to 42 and 57 °C, respectively. Even if, the increase of adsorption capacity was insignificant which was only by 3.45 and 7.69% at 42 and 57 °C, respectively, the chemical adsorption should be more than physical adsorption on the AC-MABB0.4 according to Le Chatelier's principle [42]. Further investigation was highlighted in the adsorption kinetics and isotherm studies.
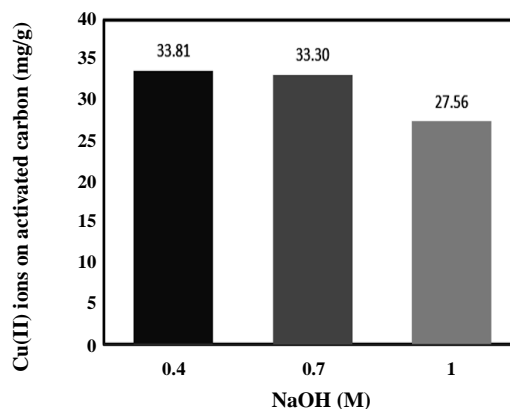

Fig. 5: Cu(II) on activated carbon over NaOH concentration for activation.
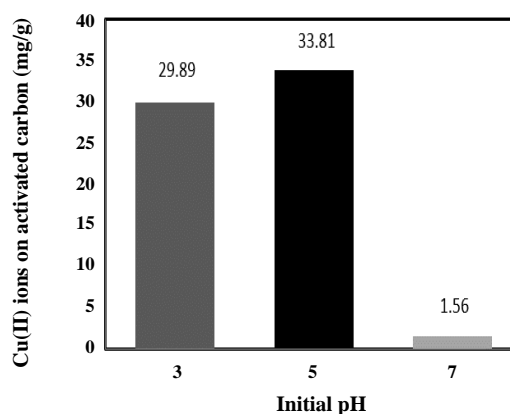

Fig. 6: Cu(II) on activated carbon over the initial pH of the solution.
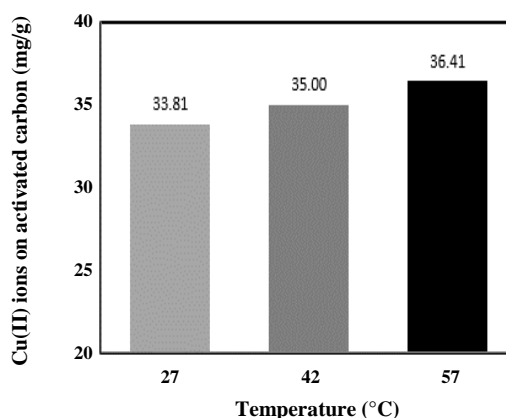

Fig. 7: Cu(II) on activated carbon over initial Cu(II) ions concentration.

Research Article

Adsorption kinetics and isotherm of the AC-MABB0.4

The linearized Lagergren model of Pseudo-First-Order Kinetic (PFOK) is given in Equation (1), and the linearized Ho model of Pseudo-Second-Order Kinetic (PSOK) is given as Eq. (2) [27,30,39].

$$\log(q_e - q_t) = \log q_e - \left(\frac{k_L t}{2.303}\right) \tag{1}$$

$$\frac{t}{q_t} = \frac{t}{k_H q_e^2} + \frac{1}{q_e} \tag{2}$$

where q_t denotes as the AC-MABB0.4 adsorption capacity (mg/g) at the time (min) of t; q_e is the q_t value at equilibrium (e) time; k_L is the adsorption rate constant (/min) for the PFOK model; and k_H (g/mg.min) is the PSOK adsorption rate constant. The adsorption kinetics system consisted of 100 mL Cu(II) ions solution at 511.32 mg/L, pH 5, 27, and 57 °C, 1 g of the AC-MABB0.4, 0–120 min contact time, 100-rpm stirring speed, and 1 atm. All the constant values of the PFOK and PSOK model were obtained by using the slope and interception of Eqs (1) and (2), respectively.

The optimum condition-based adsorption kinetic are being referred to as the maximum adsorption capacity at 57 °C and 27 °C as highlighted in the previous section. As the plot reveals and shown in Fig. 8, the PSOK model gives the best fitting to the AC-MABB0.4 adsorption kinetic with a higher correlation coefficient, and the R^2 value of 0.995 and 0.999 at 27 and 57 °C, respectively.

The Langmuir isotherm and Freundlich isotherm models were also used in this present work, and the linearized form is written in Eqs. (3) and (4) [27, 30, 39]:

$$\frac{C_e}{q_t} = \frac{1}{q_m K_L} + \frac{1}{q_m} C_e \tag{3}$$

$$\log q_e = \frac{1}{n} \log C_e + \log K_F \tag{4}$$

Where C_e (mg/L) and q_m (mg/g), is the equilibrium time-based Cu (II) ions concentration in the solution and the Langmuir-based adsorption capacity, respectively; K_L (L/mg) and K_F (L/mg) denote the constant of Langmuir and Freundlich isotherm, respectively; and $1/n$ is the Freundlich-based intensity of the adsorption. All the constant values were obtained by the slope
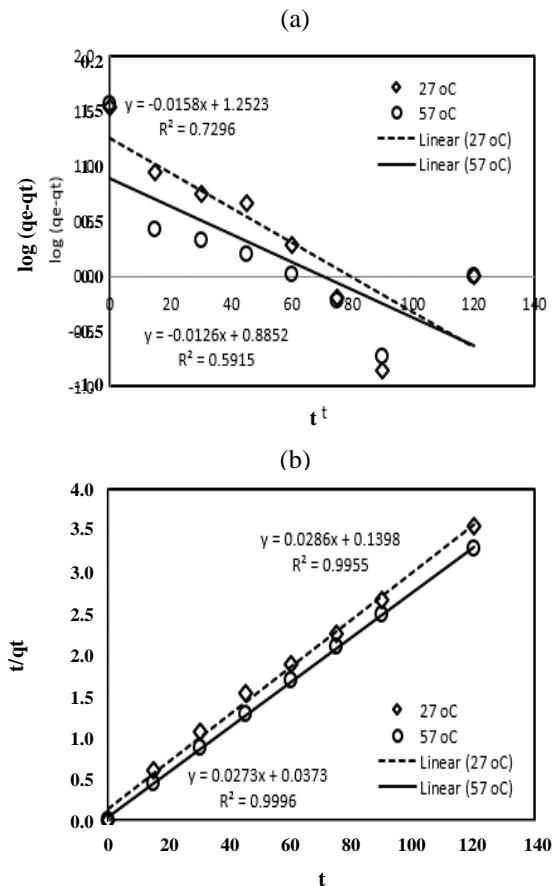

Fig. 8: Adsorption kinetic plots for the linearized (a) PFOK model and (b) the PSOK model.

and the interception of Equations (3) and (4), respectively.

Fig. 9 shows the best fitting which was obtained by Langmuir isotherm with the R^2 value of 0.981 and 0.991 at 27 and 57 °C, respectively. The Langmuir isotherm was reasonable for this case because the adsorbate monolayer on the adsorbent surface is generally related to pseudo-second-order kinetic adsorption [19, 27, 43]. As expected in the previous discussion, the rise in adsorption, the temperature increased insignificantly the AC-MABB0.4 adsorption capacity. Table 1 shows the increment of the adsorption capacity is only by 4.76% and 14.28% based on the PSOK model and Langmuir model respectively.

Cu(II) adsorption capacity by various activated carbon

Table 2 shows lignocellulosic materials-based activated carbon including the sample of Musa Acuminata

Tabel 1: The adsorption kinetic and isotherm constants.

	The PSOK Model			Langmuir Model		
	q_e	K_H	R^2	q_m	K_L	R^2
27 °C	34.965	0.006	0.999	40.322	0.031	0.981
57 °C	36.630	0.020	0.999	46.082	0.026	0.991

Table 2: A comparison of lignocellulosic materials-based activated carbon for Cu(II) ions.

| Lignocellulosic materials	Activator	T (°C)	pH	q_m (mg/g)	Ref.
Hazelnut husks	$ZnCl_2$	18	5.7	6.650	[21]
Hazelnut shell	H_2SO_4	50	6	58.270	[23]
Tunisian date stones	H_3PO_4	40	5	31.250	[25]
Australian pine-cone	NaOH	25	5	26.710	[27]
Pithecellobium jiringa	NaOH	27	5	104.167	[28]
Areca catechu shell	NaOH	27	6.5	50.51	[38]
Areca catechu shell	NaOH	45	6.5	55.25	[38]
Watermelon	$Ca(OH)_2$	30	5	31.025	[40]
Watermelon	$C_6H_8O_7$	30	5	27.027	[40]
Apricot stone	H_2SO_4	NA	6.5	22.800	[44]
Musa Acuminata banana bunch	NaOH	27	5	40.322	present study
Musa Acuminata banana bunch	NaOH	57	5	46.082	present study
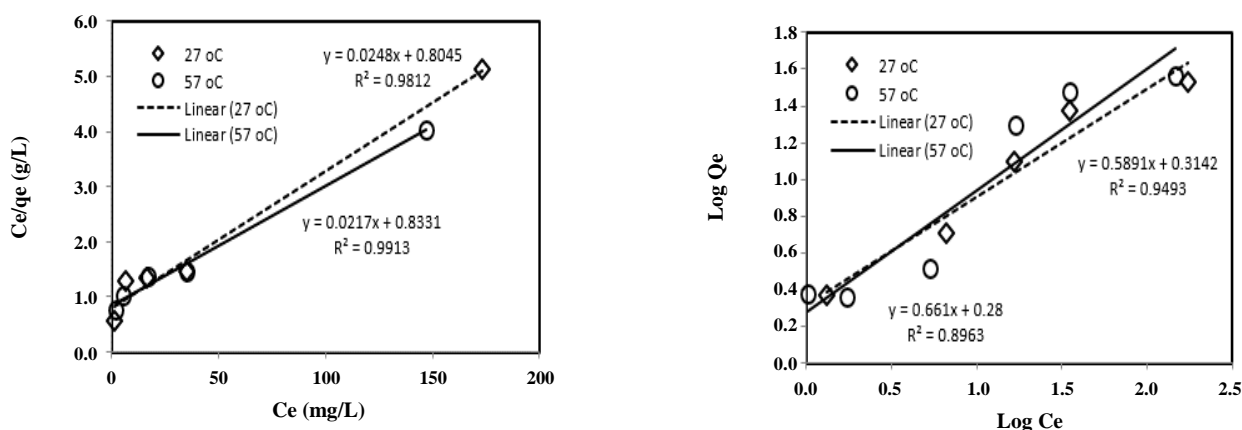
Fig. 9: Adsorption isotherms plots for (a) Langmuir isotherm (b) Freundlich isotherms.

banana bunch in the present study (the AC-MABB0.4) for Cu(II) ions for different adsorption conditions. From Table 2, it is apparent that the AC-MABB0.4 adsorption capacity is more as compared to those prepared from hazelnut husks, Tunisian date stones, Australian pine-cone, Watermelon, and Apricot stone. However, it is lower than those prepared from Hazelnut shell, areca catechu shell, and Pithecellobium jiringa.

CONCLUSIONS

This study proposed the preparation of Musa Acuminata banana bunch-based activated carbon (AC-MABB)

via physical and chemical activations. The FT-IR and SEM analyses were conducted to investigate the active sites and morphology structure of the activated carbon, respectively. The Cu(II) ions adsorption performance investigations of AC-MABB were conducted in a batch mode experiment, and the optimum adsorption condition for 1 g of the AC-MABB was observed to be under 0.4 M NaOH activation atmosphere and, stirred at initial pH of 5 with a speed of 100-rpm and a pressure of 1 atm. The Cu(II) ions adsorbed onto the AC-MABB showed excellent fitting to the pseudo-second-order adsorption kinetic with a correlation coefficient value of 0.999. Meanwhile, it followed Langmuir isotherm with coefficient values of 0.981 and 0.991 at 27 and 57 ℃, respectively. The maximum Cu(II) ions adsorption capacity based on Langmuir was approximately 40.322 and 46.082 mg/g at 27 and 57 ℃, respectively. In this investigation, it is found out that the adsorption performance of AC-MABB is comparable to other lignocellulosic materials-based activated carbon and could be an option as the adsorbent in removing heavy metal in soil and wastewater.

REFERENCES

[1] Ahmad K.S., Evaluating the Adsorption Potential of Alachlor and its Subsequent Removal from Soils *via* Activated Carbon, *Soil Sediment Contam.: Int. J.*, **27(4)**: 249-266 (2018).

[2] Hawkes S.J., What is a "Heavy Metal"? *J. Chem. Educ.*, **74(11)**: 1374-1380 (1997).

[3] Bala M., Shehu R.A., Lawal M., Determination of the Level of Some Heavy Metals in Water Collected from Two Pollution – Prone Irrigation Areas Around Kano Metropolis, *J. Pure Appl. Sci.*, **1(1)**: 6-38 (2008).

[4] Srivastava N.K., Majumder B.C., Novel Biofiltration Methods for the Treatment of Heavy Metals from Industrial Wastewater, *J. Hazard Mater.*, **151(1)**: 1-8 (2008).

[5] Yan-Biao G., Hong F., Chong C., Chong-Jian J., Fan X., Ying L., Heavy Metal Concentrations in Soil and Agricultural Products Near an Industrial District, *Pol. J. Environ. Stud.*, **22(5)**:1357-1362 (2013).

[6] Lakherwal D., Adsorption of Heavy Metals: A Review, *Int. J. Environ. Res. Dev. (I.J.E.R.D.)*, **4(1)**: 41-48 (2014).

[7] Minamisawa M., Minamisawa H., Yoshida S., Takai N., Adsorption Behavior of Heavy Metals on Biomaterials, *J. Agr. Food Chem.*, **52(18)**: 5606-5615 (2004).

[8] Theophanides T., Anastassopoulou J., Copper and Carcinogenesis. Critical Reviews in Oncology/Hematology, *J. Crit. Rev. Oncol./Hematol*. **42(1)**: 57-64 (2002).

[9] Carl L.K., Harry J.M., Elizabeth M.W., "A Review: The Impact of Copper on Human Health", International Copper Association Ltd., New York USA (2005).

[10] Ahmad K.S., Sorption and Juglans Regia-Derived Activated Carbon-Mediated Removal of Anilinebased Herbicide Alachlor from Contaminated Soils, *Environ. Earth Sci.*, **77(12)**: 437-445 (2018).

[11] Eccles H., Treatment of Metal-Contaminated Wastes: Why Select a Biological Process?, *Trends Biotechnol.*, **17(12)**: 462-465 (1999).

[12] Leung W.C., Wong M.F., Chua H., Lo W., Yu P.H.F., Leung C.K., Removal and Recovery of Heavy Metals by Bacteria Isolated From Activated Sludge Treating Industrial Effluents and Municipal Wastewater, *Water Sci. Technol.*, **41(12)**: 233-240 (2000).

[13] Basso M.C., Cerrella E.G., Cukierman A.L., Lignocellulosic Materials as Potential Biosorbents of Trace Toxic Metals from Wastewater, *Ind. Eng. Chem. Res.*, **41(15)**: 3580-3585 (2002).

[14] Wong K.K., Lee C.K., Low K.S., Haron M.J., Removal of Cu and Pb by Tartaric Acid Modified Rice Husk From Aqueous Solutions, *Chemosphere*, **50**: 23-28 (2003).

[15] Benaïssa H., Elouchdi M.A., Removal of Copper Ions from Aqueous Solutions by Dried Sunflower Leaves, *Chem. Eng. Process.*, **46**: 614-622 (2007).

[16] Dang V.B.H., Doan H.D., Dang-Vu T., Lohi A., Equilibrium and Kinetics of Biosorption of Cadmium (II) and Copper (II) Ions by Wheat Straw, *Bioresour. Technol.*, **100**: 211-219 (2009).

[17] Chen H., Dai G., Zhao J., Zheng A., Wu J., Yan H., Removal of Copper(II) Ions by a Biosorbent-Cinnamomum Camphora Leaves Powder, *J. Hazard. Mater.*, **177**: 228-336 (2010).

[18] Pehlivan E., Altun T., Parlayici S., Modified Barley Straw as a Potential Biosorbent for Removal of Copper Ions, *Food Chem.*, **135**: 2229-2234 (2012).

[19] Muslim A., Zulfian, Ismayanda M.H., Devrina E., Fahmi H., Adsorption of Cu(II) from the aqueous Solution by Chemical Activated Adsorbent of Areca Catechu Shell, *J. Eng. Sci. Technol.*, **10**(12): 1654-1666 (2015).

[20] https://www.alliedmarketresearch.com/activated-carbon-market.

[21] Imamoglu M., Tekir O., Removal of Copper (II) and Lead (II) Ion from Aqueous Solution by Adsorption on Activated Carbon from a New Precursor Hazelnut Husks, *Desalination*, **228(1-3)**: 108-113 (2008).

[22] Klasson K.T., Wartelle L.H., James E., Rodgers J.E., Lima I.M., Copper(II) Adsorption by Activated Carbons from Pecan Shells: Effect of Oxygen Level During Activation, *Ind. Crops. Prod.*, **30(1)**: 72-77 (2009).

[23] Demirbas E., Dizge N., Sulak M.T., Kobya M., Adsorption Kinetic and Equilibrium of Copper from Aqueous Solution Using Hazelnut Shell Activated Carbon, *Chem. Eng. J.*, **148(2-3)**: 480-487 (2009).

[24] Moreno-Pirajan J.C., Giraldo L., Adsorption of copper from Aqueous Solution by Activated Carbons Obtained by Pyrolysis of Cassava Peel, *J. Anal. Appl. Pyrol.*, **87(2)**: 188-193 (2010).

[25] Bouhamed F., Elouear Z., Bouzid J., Adsorptive Removal of Copper(II) from Aqueous Solution on Activated Carbon Prepared from Tunisian Date Stones: Equilibrium, Kinetic and Thermodynamics, *J. Taiwan Inst. Chem. E.*, **43(5)**: 741-749 (2012).

[26] Milenković D.D., Bojić A.L.J., Veljković V.B., Ultrasound-Assisted Adsorption of 4-Dodecylbenzene Sulfonate from Aqueous Solution by Corn Cob Activated Carbon, *Ultrason. Sonochem.*, **20(3)**: 955-962 (2013).

[27] Muslim A., Australian Pine Cones-Based Activated Carbon for Adsorption of Copper in Aqueous Solution, *J. Eng. Sci. Technol.*, **12(2)**: 280-295 (2017).

[28] Muslim A., Ellysa, Syahiddin D.S., Cu(II) Ions Adsorption Using Activated Carbon Prepared from Pithecellobium Jiringa (Jengkol) Shells with Ultrasonic Assistance: Isotherm. Kinetic and Thermodynamic Studies, *J. Eng. Tech. Sci. (J.E.T.S.)*, **49(4)**: 472-490 (2017).

[29] Syahiddin D.S., Muslim A., Adsorption of Cu(II) Ions onto Myristica Fragrans Shell-Based Activated Carbon: Isotherm, Kinetic and Thermodynamic Studies, *J. Korean Chem. Soc.*, **62(2)**: 79-86 (2018).

[30] Muslim A., Marwan, Saifullah R., Azwar M.Y., Darmadi, Putra B.P., Rizal S., Adsorption of Cu(II) Ions on Areca Catechu Stem-based Activated Carbon: Optimization Using Response Surface Methodology, *Int. Rev. Model. Simul. (I.R.E.M.O.S.)*, **12(2)**: 123-129 (2019).

[31] Sugumaran P., Susan V.P., Ravichandran P., Seshadri S., Production and Characterization of Activated Carbon from Banana Empty Fruit Bunch and Delonix Regia Fruit Pod, *J. Sustain. Ener. & Environ.*, **3**: 125-132 (2012).

[32] Adebisi G.A., Chowdhury Z.Z., Abd Hamid S.B., Ali E., Hydrothermally Treated Banana Empty Fruit Bunch Fiber Activated Carbon for Pb(II) and Zn(II) Removal, BioResources, **11**(4): 9686-9709 (2016).

[33] http://www.fao.org/economic/est/est-commodities/bananas/bananafacts/en/#.XvJHsOfLfIW.

[34] Hesas R.H., Daud W.M.A.W., Sahu J.N., Arami-Niya A., The Effects of a Microwave Heating Method on the Production of Activated Carbon from Agricultural Waste: A Review, *J. Anal. Appl. Pyrolysis*, **100**: 1-11 (2013).

[35] Chakravarty P., Sarma N.S., Sarma H.P., Removal of Lead(II) from Aqueous Solution Using Heartwood of Areca Catechu Powder, *Desalination*, **256**: 16-21 (2010).

[36] Figueiredo J.L., Pereira M.F.R., Freitas M.M.A., Qrfao, J.J.M., Modification of the Surface Chemistry of Activated Carbons, *Carbon*, **37(9)**: 1379-1389 (1999).

[37] Mengistie A.A., Siva R.T., Prasada R.A.V., Singanan M., Removal of Lead(II) Ion from Aqueous Solution Using Activated Carbon from Militia Ferruginea Plant Leaves, *Bull. Chem. Soc. Ethiop.*, **22(3)**: 349-360 (2008).

[38] Muslim A., Aprilia S., Suha T.A., Fitri Z., Adsorption of Pb(II) Ions from Aqueous Solution Using Activated Carbon Prepared from Areca Catechu Shell: Kinetic, Isotherm and Thermodynamic Studies, *Korean Chem. Soc.*, **61(3)**: 1017-2548 (2017).

[39] Muslim A., Optimization of Pb(II) Adsorption onto Australian Pine Cones-Based Activated Carbon by Pulsed Microwave Heating Activation, *Iran. J. Chem. Chem. Eng. (IJCCE)*, **36(5)**: 115-127 (2017).

[40] Gupta H., Gogate P.R., Intensified Removal of Copper from Waste Water Using Activated Water Melon Based Biosorbent in the Presence of Ultrasound, *Ultrason. Sonochem.*, **30**: 113-122 (2016).

[41] Runtti H., Tuomikoski S., Kangas T., Lassi U., Kuokkanen T., Rämö J., Chemically Activated Carbon Residue from Biomass Gasification as a Sorbent for Iron(II), Copper(II) and Nickel(II) Ions, *J. Water Process. Eng.*, **4**: 12-24 (2014).

[42] Rao S.R., "Surface Chemistry of Froth Flotation: Volume 1: Fundamentals", Springer Science, New York USA (2004).

[43] Kiran B., Thanasekaran K., Copper Biosorption on Lyngbya Putealis: Application of Response Surface Methodology (RSM), *Int. Biodeter. Biodegr*., **65(6)**: 840-845 (2011).

[44] Kobya M., Demirbas E., Senturk E., Ince, M., Adsorption of Heavy Metal Ions from Aqueous Solutions by Activated Carbon Prepared from Apricot Stone, *Bioresour. Technol*., **96(13)**: 1518-1521 (2005).